Following Adsorption Kinetics at Electrolyte/Metal Interfaces through Crystal Truncation Scattering: Sulfur on Au(111)

C. Vericat, M. E. Vela, G. A. Andreasen, and R. C. Salvarezza
Instituto de Investigaciones Fisicoquímicas Teóricas y Aplicadas (INIFTA), (CIC-CONICET-UNLP), La Plata, Argentina

F. Borgatti and R. Felici
INFM-OGG, c/o ESRF, BP 220 Grenoble, France

T.-L. Lee, F. Renner, and J. Zegenhagen
European Synchrotron Radiation Facility, BP 220, F-38043 Grenoble, France

J. A. Martín-Gago
Instituto Ciencia de Materiales de Madrid-CSIC, Cantoblanco 28049-Madrid, Spain
(Received 29 August 2002; published 21 February 2003)

Combining electrochemical methods, *in situ* scanning tunneling microscopy, and surface x-ray diffraction allowed study of the structure and kinetics of S/Au(111) electrodes in aqueous electrolytes under potential control. Integrated intensities of a particular crystal truncation rod at anti-Bragg conditions were used to trace the sulfur adsorption and desorption as a function of electrode potential in real time. The S desorption is a first order process and the adsorption follows a Langmuir isotherm. A weakly bound S layer is found on the surface *before* charge transfer, and then specific adsorption occurs.

DOI: 10.1103/PhysRevLett.90.075506 PACS numbers: 68.43.Mn, 61.10.–i, 68.37.Ef, 81.15.Lm

The understanding of the surface structure of the first atomic layers of crystals has attracted considerable attention because their atomic arrangement determines the electronic properties and reactivity of surfaces. The ability to control the surface structure at the atomic level is a crucial point, not only for designing new materials for catalytic applications, but also in the development of the rapidly developing wide field of nanotechnology [1].

Sulfur (S) and S-containing organic molecules adsorbed on metals represent very interesting systems, as S is a well-known poison in heterogeneous catalysis [2], and S-containing organic molecules, such as alkanethiols, play a key role in nanotechnology applications [3]. Therefore, these species adsorbed on well-defined metal surfaces, particularly the Au(111) face, have been taken as a model system for interfacial science research [4]. Since many of the technological implications of these species involve aqueous electrolytes, a complete description of the atomic structure of the electrolyte/S-covered Au(111) interface deserves special interest. Furthermore, a true atomistic description of the electrolyte/electrode interface requires, in addition to electrochemical techniques, the use of *in situ* structural methods, in particular, scanning probe microscopies (SPM) and surface x-ray diffraction (SXRD). While these types of combined studies have been done for relatively simple systems [5], they have not been used to characterize more complex systems such as the adsorption of S and S-containing organic molecules.

In this Letter we present a combined electrochemical, *in situ* scanning tunneling microscopy (STM) and SXRD study of Au(111)/S electrodes in aqueous electrolytes. The integrated intensity in anti-Bragg conditions of a particular crystal truncation rod (CTR) has been used to follow changes in the amount of adsorbed species induced by the electrode potential in real time [5]. Thus, we were able to identify weakly bound S species before anodic adsorption or after cathodic stripping. Furthermore, we could follow the kinetics of the adsorption/desorption processes in real time. We have extended our study to alkanethiol adsorption on the same substrate with similar results and conclusions.

In situ SXRD was performed at the insertion device beam line ID32 at the ESRF in Grenoble, France using a wavelength of $\lambda = 0.118$ nm. A flame-annealed Au(111) single crystal was used for the experiments. The Au(111) was mounted on a Kel-F electrochemical cell similar to that described in Ref. [6], fitted with a miniature, leak-tight Ag/AgCl as reference and a Pt counter electrode. X-ray passage was permitted by a mylar window, which could be inflated (thick-film electrolyte) or deflated (thin-film electrolyte) by adjusting the electrolyte pressure [6]. The angle of incidence was 1°, i.e., above the critical angle. *In situ* STM images were taken with a Nanoscope III by using (111) preferred oriented vapor deposited Au films on glass substrates. Typical tunneling current and bias voltage were 20 nA and 0.3–0.4 V, respectively. The electrolyte, 0.1 M NaOH + 10^{-3} M Na_2S (suprapure and Milli-Q water), was deaerated for 2 h with pure nitrogen.

A typical voltammogram, i.e., current density (j) vs E plot for an Au(111) single crystal in 0.1 M NaOH + 10^{-3} M Na_2S, is shown in Fig. 1 (top curve), which was obtained in the electrochemical cell where *in situ* x-ray

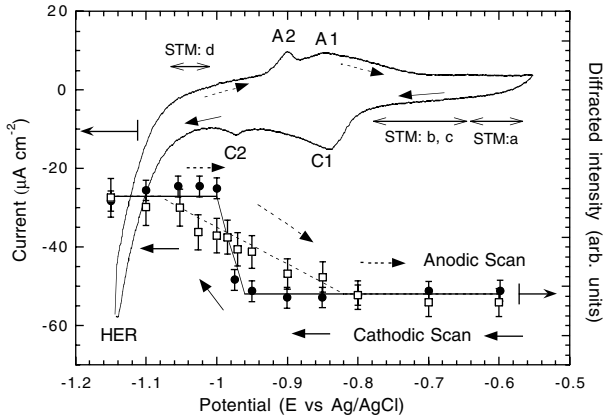

FIG. 1. (Upper curve, left axis) Cyclic voltammogram for Au(111) in 0.1 M NaOH + 10^{-3} M Na_2S. Sweep rate was 0.001 V/s. The labels STM (a)–(d) correspond to the STM images in Fig. 2. (Lower curve, right axis) Integrated diffraction intensity at (HKL) = (1 0 2.5) as a function of the applied voltage in a cathodic (solid circles) and anodic scan (empty squares). The lines are fitted to the data as a guide for the eye. Dotted arrows indicate anodic scan direction, and solid arrows cathodic scan direction.

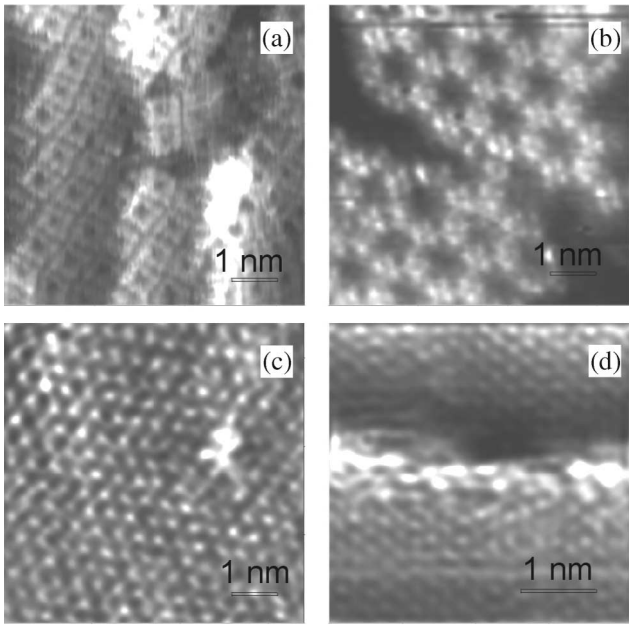

FIG. 2. *In situ* atomic resolution STM images recorded at electrode potentials shown by the arrows in Fig. 1.

diffraction measurements were performed [6]. In the cathodic sweep (C direction) a peak at -0.84 V ($C1$) and a small one at -0.97 V ($C2$) can be identified prior to hydrogen evolution (HER), which starts at about -1.05 V. The anodic sweep (A direction) reveals a peak at -0.9 V ($A2$) and a broad one ($A1$) at about -0.84 V. *In situ* STM measurements [7] had shown that in the potential range $-0.65\ \text{V} < E < -0.55\ \text{V}$, the main species present on the surface are S octomers (S_8) [Fig. 2(a)]. In the C direction, within the range $-0.78 < E < -0.65$ V, domains of S trimers (S_3) are imaged by the STM [Fig. 2(b)]. Eventually, however, at -0.78 V S_8 and S_3 species are slowly transformed into monomeric S and a small fraction of the S atoms go to solution while the remaining ones rearrange slowly into a $(\sqrt{3} \times \sqrt{3})R30°$ lattice [Fig. 2(c)] [7]. Thus, in this potential range, the $(\sqrt{3} \times \sqrt{3})R30°$ lattice, S_3 and S_8 structures coexist. The free energies of the structures must be similar and the slow kinetics of the structural transition results in a complex surface consisting of rather small, only locally ordered domains. STM results [7] suggest that all the sulfur is stripped from the terraces at -0.84 V ($C1$, Fig. 1) and that at $E = -1.05$ V, a 1×1 Au(111) surface structure is observed. Only a few S atoms remain adsorbed at step edges [Fig. 2(d)] [7]. STM experiments indicate complete stripping of S at potentials negative of the small peak ($C2$) preceding HER. In the A direction this behavior is reversed: S species from solution first adsorb at step edges (peak $A2$), then on terraces, leading to the $(\sqrt{3} \times \sqrt{3})R30°$ sulfur lattice (broad peak $A1$), and finally at $E > -0.80$ V, the $(\sqrt{3} \times \sqrt{3})R30°$ lattice slowly transforms into S_3 and S_8 species [7,8].

X-ray diffraction data collected at the same potential conditions did not show any fractional order diffraction spots. This can be understood since the surface is covered with small domains of different sulfur species, arranged in different lattices (STM images, Fig. 2). Surface structural information still can be obtained by measuring different CTRs [9] of the Au(111) surface at given E values. In the following, we use hexagonal coordinates for the reciprocal space with the l direction normal to the Au(111) surface. In Fig. 3 we show the (1 0 L) CTRs obtained for $E = -0.76$ V and $E = -1.05$ V, corresponding to the regions of the voltammogram where the S layer is on the surface and after it has been stripped to the solution, respectively. These rods have been obtained at specific E by integrating rocking scans, i.e., ω scans. The shapes of the two CTRs are clearly different, in particular, concerning the positions of the minima, as a

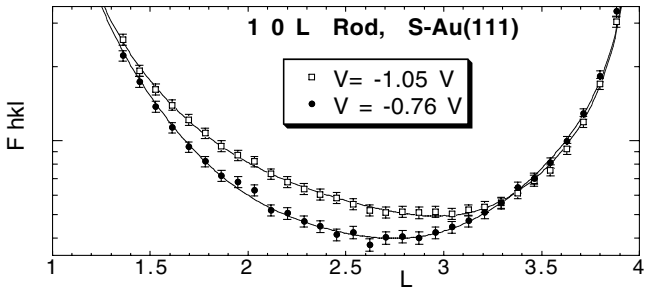

FIG. 3. (1 0 L) CTR for Au(111) in 0.1 M NaOH + 10^{-3} M Na_2S recorded at two different electrode potentials. The overlapping solid lines represent the best fit. The difference between the curves is due to the presence of a S layer.

result of a change in surface structures. These CTRs were measured subsequently on the same sample and the changes were reversible. The solid lines are the best fit to the data obtained using the rod program [10]. The χ^2 values are 0.38 and 0.66, for the CTRs recorded at $E = -1.05$ and -0.76 V, respectively. The aim of the fit was to appreciate the relative parameters that account for the differences between them rather than to perform a complete structural determination, which would require a much more extensive data set. The data collected at $E = -1.05$ V correspond to clean Au(111). The fit has been obtained with Au atoms in their bulk positions, with no surface roughness, and using the Debye-Waller factors as free parameters. The experimental data, and consequently the fit parameters, are very similar to the values determined for clean Au(111) measured under UHV conditions [11], indicating that by electrochemical methods it is possible to obtain surface qualities similar to those attained under UHV conditions. The rod shape at $E = -0.76$ V could be satisfactorily reproduced only by introducing a S layer at a vertical distance of 0.23 ± 0.01 nm with respect to the last Au(111) layer. The best fit was obtained with the S atoms in fcc hollow positions and with a total coverage $\theta \approx 1/3$ ML. These values match well with the predominant $(\sqrt{3} \times \sqrt{3})R30°$ surface structure observed by STM. The last Au layer was found to expand about 0.067 ± 0.005 nm (+ 2.85%) with respect to bulk Au(111) [12]. Therefore, we conclude that CTR shape, and particularly the difference between minima in the rods, is a sensitive measure of θ and that the central part of the rod shifts up when all the S is stripped.

We have verified that the CTRs measured from a clean Au(111) surface immersed in 0.1 M NaOH do not show any dependence on E. In this case, all the CTRs overlap the experimental points for S-Au(111) at $E = -1.05$ V (Fig. 3, upper curve). This proves that the CTR obtained at this potential corresponds to a clean Au(111) surface in agreement with STM images. The CTR shapes are very similar to those measured in UHV conditions [11], providing further evidence that the CTR at -1.05 V represents a clean gold surface.

Taking advantage of the strict relation between θ and the diffracted intensity, we recorded ω scans at the point of the rod which is most sensitive to the presence of the S layer (i.e., at $L = 2.5$ r.l.u.) while changing E and simultaneously recording a voltammogram, as shown in Fig. 1, starting from $E = -0.6$ V. In Fig. 1 we plot the integrated diffraction peak intensities as a function of the potential, which we call *cyclic diffractogram* [13]. In the C direction, we observe two well-defined regions where the diffraction intensity is almost constant, separated by a sudden rise that takes place when E reaches -0.98 V. These two potential regions correspond to E values where the STM pictures show the presence or the absence of adsorbed S on the Au(111) terraces. Therefore, this way of measuring the diffraction intensity is a suitable method of following the S coverage as a function of E in real time. The absorption/desorption process is reversible. Figure 4 shows the intensity at the CTR minimum with time, while cycling the potential. The starting potential was -0.476 V, then it was scanned at a speed of 0.005 V/s and reversed when E reached the value of -1.1 V. The arrows indicate the time where the voltage scan is reversed (i.e., changed from C to A direction). S atoms leave the surface to the solution and reattach at the surface, and after each complete process the diffraction intensity recovers its original value, proving the absence of roughening of the Au(111) surface, which appears to react completely elastically. The system can be cycled some tens of times before observing irreversibility associated with a roughening of the surface. Similar scans made in 0.1 M NaOH (in the absence of sulfur species) show no such change.

The information derived from the CTRs and cyclic voltammetry give valuable insight into the nature of the adsorption and the kinetics of the adsorption/desorption process. An important observation derived from Fig. 1 is that the rise in the *cyclic diffractogram* (at -0.98 V) appears 0.1 V shifted from the main desorption peak in the voltammogram (at -0.85 V). The fact that the diffraction intensity suddenly changes at potential values where chemisorbed sulfur has already been completely transformed into sulfide anions (peak $C1$) suggests that these species remain on the Au(111) surface, supposedly in a more weakly bound state, which may be a physisorbed state. Note that the increase in the diffraction intensity coincides with the potential range of the small peak ($C2$) preceding hydrogen evolution reaction. This suggests that this peak may not only reflect the charge transfer due to S electrodesorption from step edges (as previously derived from STM images and Ref. [8]), but also some change in the capacitive charge of the Helmhotz layer because of the rearrangement of the

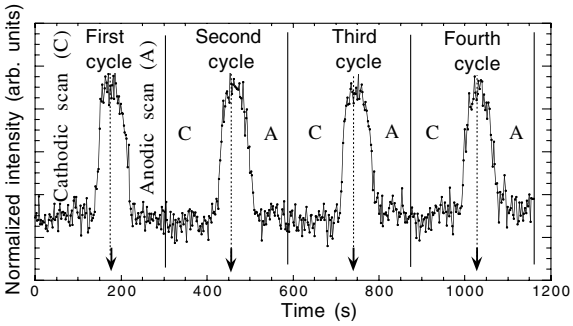

FIG. 4. Real-time measurement of the evolution of the diffracted intensity at (1 0 2.5). The diffraction peak was recorded while scanning the electrode potential at 0.005 V/s. The arrows mark the time where the scan is reversed. The starting and reversing potentials are -0.476 and -1.1 V, respectively.

electrochemical double layer due to the desorption of the weakly bound sulfide.

The same behavior is observed during sulfide readsorption, where the diffraction intensity decays to a minimum well before chemisorption takes place at peak $A1$. The weakly bound state cannot be easily detected by electrochemical techniques, since no charge transfer is involved, and is also not visible in the STM images [14]. Therefore, the combination of diffraction intensity vs E with current density vs E data is a powerful tool to discriminate between the different chemical states of the adsorbate. It should be mentioned that the existence of weak adsorbed S species had been proposed from surface enhanced Raman scattering measurements [15] and electroreflectance spectroscopy [16] for polycrystalline Au, but no evidence of this state had been found for well-defined single crystal faces. Here, we have obtained clear-cut evidence that sulfur chemisorption on Au(111) surfaces is preceded by an adsorption step, possibly physisorption. The layer of negatively charged sulfide should be stabilized on the Au surface by water or Na^+ coadsorption [16], as has been also observed for I^- adsorption on Au(111) in Cs^+-containing solutions [17].

Now we discuss the kinetics involved in the physisorption process. The fact that the *cyclic diffractogram* exhibits a discontinuity in the negative scan strongly suggests that the removal of the weakly bound sulfide layer involves a first order phase transition [18]. This means that when the negative charge of the Au surface reaches a critical value the negatively charged sulfide layer is completely removed from the surface. On the other hand, the weak adsorption of sulfide and Na^+ species from the solution increases smoothly with E, i.e., as the negative charge of the Au(111) surface decreases. The shape of the diffraction intensity plot fits a Langmuir isotherm reasonably well.

Finally, we have recorded similar *cyclic diffractograms* for the hexanethiol/Au(111) interface in 0.1 M NaOH (previously assembled in 0.1 mM ethanolic solution), obtaining similar results, i.e., we are able to observe a 0.1 V shift in the desorption energy allowing us to conclude the existence of an ionic, possibly physisorbed hexanethiol state. Although such a physisorbed state has been proposed for alkanethiolate adsorption on Au(111) by spectroscopy data [19], the relative contribution of the hydrocarbon chains and sulfur heads to this state is not clear. Our results demonstrate that the physisorbed state is mediated mainly by the sulfur head rather than by the hydrocarbon chains, which would only contribute to its stabilization. The fact that S and alkanethiolate exhibit the same behavior is certainly interesting because it helps to understand the origin of forces that stabilize the physisorbed state in alkanethiols [19].

In summary, our results demonstrate the existence of a weakly bound, possibly physisorbed sulfur state on the Au(111) face, which resides at nearly the same distance as the chemisorbed species. The method of *cyclic diffractommetry* used in this work should be useful to investigate the existence of physisorbed states in other similar electrochemical systems as alkanethiols. Because of the high sensitivity of the used CTR diffraction technique, kinetic information about adsorption/desorption processes that is not easily accessible by electrochemical or SPM methods can be obtained.

We acknowledge L. Vazquez for useful discussions. This work has been performed within the CSIC-CONICET Programa de Cooperación con Iberoamérica and the Spanish research Project No. Mat2002-395.

[1] *Frontiers in Surface and Interface Science*, edited by C. B. Duke and E.W. Plummer (Elsevier, Amsterdam, 2002).
[2] J. A. Rodriguez and J. Hrbek, Acc. Chem. Res. **32**, 719 (1999).
[3] *Self-Assembled Monolayers of Thiols*, edited by A. Ulman, Thin Films Vol. 24 (Academic, San Diego, 1998).
[4] P. Fenter, A. Eberhardt, and P. Eisenberger, Science **266**, 1216 (1994); G. J. Jackson *et al.*, Phys. Rev. Lett. **84**, 119 (2000).
[5] J. Wang, A. J. Davenport, H. S. Isaacs, and B. M. Ocko, Science **255**, 1416 (1992).
[6] J. Zegenhagen *et al.*, Surf. Sci. **352–354**, 346 (1996).
[7] C. Vericat, G. Andreasen, M. E. Vela, and R. C. Salvarezza, J. Phys. Chem. B **104**, 302 (2000).
[8] C. Vericat *et al.*, Langmuir **17**, 4919 (2001).
[9] I. K. Robinson, Appl. Surf. Sci. **56–58**, 117 (1992).
[10] E. Vlieg, J. Appl. Crystallogr. **33**, 401 (2000).
[11] A. R. Sandy *et al.*, Phys. Rev. B **43**, 4667 (1991).
[12] J. Li, K. S. Liang, G. Scoles, and A. Ulman, Langmuir **11**, 4418 (1995).
[13] B. M. Ocko, G. M. Watson, and J. Wang, J. Phys. Chem. **98**, 897 (1994).
[14] Weakly bound species are difficult to detect by STM because (i) adsorbate/substrate interactions are not strong enough to prevent being easily moved by the STM tip, and (ii) the adlayer is highly mobile and disordered.
[15] X. Gao, Y. Zhang, and M. J. Weaver, Langmuir **8**, 668 (1992).
[16] R. O. Lezna, N. R. de Tacconi, and A. J. Arvia, J. Electroanal. Chem. **283**, 319 (1990).
[17] B. G. Bravo *et al.*, J. Phys. Chem. **95**, 5245 (1991).
[18] E. Budevski, G. Staikov, and W. J. Lorenz, *Electrochemical Phase Formation and Growth* (VCH, Weinheim, 1996).
[19] M. Byloos, H. Al-Maznai, and M. Morin, J. Phys. Chem. B **103**, 6554 (1999).